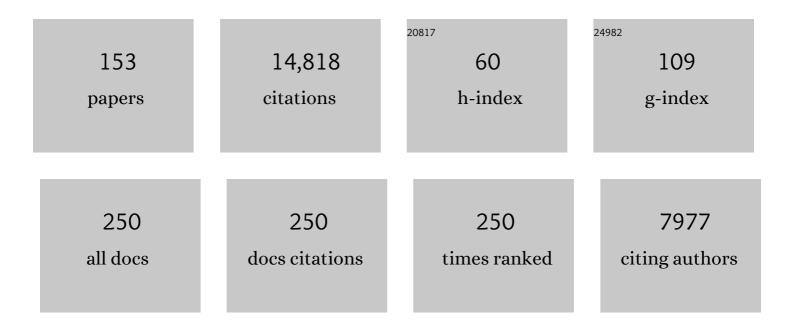
Rainer M Volkamer

List of Publications by Year in descending order

Source: https://exaly.com/author-pdf/2825398/publications.pdf Version: 2024-02-01



#	Article	IF	CITATIONS
1	O2–O2 CIA in the gas phase: Cross-section of weak bands, and continuum absorption between 297–500Ânm. Journal of Quantitative Spectroscopy and Radiative Transfer, 2022, 279, 108063.	2.3	5
2	The CU Airborne Solar Occultation Flux Instrument: Performance Evaluation during BB-FLUX. ACS Earth and Space Chemistry, 2022, 6, 582-596.	2.7	7
3	Wildfire Smoke Observations in the Western U.S. from the Airborne Wyoming Cloud Lidar during the BB-FLUX Project. Part I: Data Description and Methodology. Journal of Atmospheric and Oceanic Technology, 2022, , .	1.3	2
4	Modelling the gas–particle partitioning and water uptake of isoprene-derived secondary organic aerosol at high and low relative humidity. Atmospheric Chemistry and Physics, 2022, 22, 215-244.	4.9	8
5	Field observational constraints on the controllers in glyoxal (CHOCHO) reactive uptake to aerosol. Atmospheric Chemistry and Physics, 2022, 22, 805-821.	4.9	5
6	Quantifying Carbon Monoxide Emissions on the Scale of Large Wildfires. Geophysical Research Letters, 2022, 49, .	4.0	14
7	Survival of newly formed particles in haze conditions. Environmental Science Atmospheres, 2022, 2, 491-499.	2.4	8
8	A Comparison of Multitemporal Airborne Laser Scanning Data and the Fuel Characteristics Classification System for Estimating Fuel Load and Consumption. Journal of Geophysical Research G: Biogeosciences, 2022, 127, .	3.0	3
9	Synergistic HNO3–H2SO4–NH3 upper tropospheric particle formation. Nature, 2022, 605, 483-489.	27.8	26
10	Carbon Monoxide in Optically Thick Wildfire Smoke: Evaluating TROPOMI Using CU Airborne SOF Column Observations. ACS Earth and Space Chemistry, 2022, 6, 1799-1812.	2.7	6
11	Determination of the collision rate coefficient between charged iodic acid clusters and iodic acid using the appearance time method. Aerosol Science and Technology, 2021, 55, 231-242.	3.1	18
12	Molecular characterization of ultrafine particles using extractive electrospray time-of-flight mass spectrometry. Environmental Science Atmospheres, 2021, 1, 434-448.	2.4	10
13	Role of iodine oxoacids in atmospheric aerosol nucleation. Science, 2021, 371, 589-595.	12.6	94
14	Validation of IASI Satellite Ammonia Observations at the Pixel Scale Using In Situ Vertical Profiles. Journal of Geophysical Research D: Atmospheres, 2021, 126, e2020JD033475.	3.3	28
15	Measurement of iodine species and sulfuric acid using bromide chemical ionization mass spectrometers. Atmospheric Measurement Techniques, 2021, 14, 4187-4202.	3.1	13
16	Global tropospheric halogen (Cl, Br, I) chemistry and its impact on oxidants. Atmospheric Chemistry and Physics, 2021, 21, 13973-13996.	4.9	57
17	The driving factors of new particle formation and growth in the polluted boundary layer. Atmospheric Chemistry and Physics, 2021, 21, 14275-14291.	4.9	38
18	lodine chemistry in the chemistry–climate model SOCOL-AERv2-I. Geoscientific Model Development, 2021. 14. 6623-6645.	3.6	12

#	Article	IF	CITATIONS
19	Origin of water-soluble organic aerosols at the MaÃ⁻do high-altitude observatory, Réunion Island, in the tropical Indian Ocean. Atmospheric Chemistry and Physics, 2021, 21, 17017-17029.	4.9	4
20	Chemical composition of nanoparticles from <i>l̂±</i> -pinene nucleation and the influence of isoprene and relative humidity at low temperature. Atmospheric Chemistry and Physics, 2021, 21, 17099-17114.	4.9	12
21	Ozone depletion due to dust release of iodine in the free troposphere. Science Advances, 2021, 7, eabj6544.	10.3	5
22	Biomass burning nitrogen dioxide emissions derived from space with TROPOMI: methodology and validation. Atmospheric Measurement Techniques, 2021, 14, 7929-7957.	3.1	27
23	Global nitrous acid emissions and levels of regional oxidants enhanced by wildfires. Nature Geoscience, 2020, 13, 681-686.	12.9	51
24	Rapid growth of new atmospheric particles by nitric acid and ammonia condensation. Nature, 2020, 581, 184-189.	27.8	169
25	Photo-oxidation of Aromatic Hydrocarbons Produces Low-Volatility Organic Compounds. Environmental Science & Technology, 2020, 54, 7911-7921.	10.0	66
26	Enhanced growth rate of atmospheric particles from sulfuric acid. Atmospheric Chemistry and Physics, 2020, 20, 7359-7372.	4.9	58
27	Quantitative detection of iodine in the stratosphere. Proceedings of the National Academy of Sciences of the United States of America, 2020, 117, 1860-1866.	7.1	61
28	Molecular understanding of the suppression of new-particle formation by isoprene. Atmospheric Chemistry and Physics, 2020, 20, 11809-11821.	4.9	49
29	Characterisation of African biomass burning plumes and impacts on the atmospheric composition over the south-west Indian Ocean. Atmospheric Chemistry and Physics, 2020, 20, 14821-14845.	4.9	10
30	Molecular understanding of new-particle formation from <i>α</i> -pinene between â^'50 and +25 °C. Atmospheric Chemistry and Physics, 2020, 20, 9183-9207.	4.9	68
31	Intercomparison of NO ₂ , O ₄ , O ₃ and HCHO slant column measurements by MAX-DOAS and zenith-sky UV–visible spectrometers during CINDI-2. Atmospheric Measurement Techniques, 2020, 13, 2169-2208.	3.1	52
32	Inter-comparison of MAX-DOAS measurements of tropospheric HONO slant column densities and vertical profiles during the CINDI-2 campaign. Atmospheric Measurement Techniques, 2020, 13, 5087-5116.	3.1	18
33	Halogen activation and radical cycling initiated by imidazole-2-carboxaldehyde photochemistry. Atmospheric Chemistry and Physics, 2019, 19, 10817-10828.	4.9	12
34	Molecular Composition and Volatility of Nucleated Particles from α-Pinene Oxidation between â^50 °C and +25 °C. Environmental Science & Technology, 2019, 53, 12357-12365.	10.0	32
35	Effect of sea salt aerosol on tropospheric bromine chemistry. Atmospheric Chemistry and Physics, 2019, 19, 6497-6507.	4.9	36
36	Importance of reactive halogens in the tropical marine atmosphere: aÂregional modelling study using WRF-Chem. Atmospheric Chemistry and Physics, 2019, 19, 3161-3189.	4.9	36

#	Article	IF	CITATIONS
37	Separation of Methane Emissions From Agricultural and Natural Gas Sources in the Colorado Front Range. Geophysical Research Letters, 2019, 46, 3990-3998.	4.0	34
38	Update of the HITRAN collision-induced absorption section. Icarus, 2019, 328, 160-175.	2.5	105
39	Simulating the Weekly Cycle of NO x â€VOCâ€HO x â€O 3 Photochemical System in the South Coast of California During CalNexâ€2010 Campaign. Journal of Geophysical Research D: Atmospheres, 2019, 124, 3532-3555.	3.3	8
40	Chemistry of Volatile Organic Compounds in the Los Angeles Basin: Formation of Oxygenated Compounds and Determination of Emission Ratios. Journal of Geophysical Research D: Atmospheres, 2018, 123, 2298-2319.	3.3	43
41	Multicomponent new particle formation from sulfuric acid, ammonia, and biogenic vapors. Science Advances, 2018, 4, eaau5363.	10.3	164
42	Stratospheric Injection of Brominated Very Shortâ€Lived Substances: Aircraft Observations in the Western Pacific and Representation in Global Models. Journal of Geophysical Research D: Atmospheres, 2018, 123, 5690-5719.	3.3	36
43	The Convective Transport of Active Species in the Tropics (CONTRAST) Experiment. Bulletin of the American Meteorological Society, 2017, 98, 106-128.	3.3	50
44	Erratum to "Rayleigh scattering cross-section measurements of nitrogen, argon, oxygen and airâ€J Quant Spectrosc Radiat Transf 147 (2014) 171–177. Journal of Quantitative Spectroscopy and Radiative Transfer, 2017, 189, 281-282.	2.3	13
45	UV photochemistry of carboxylic acids at the airâ€sea boundary: A relevant source of glyoxal and other oxygenated VOC in the marine atmosphere. Geophysical Research Letters, 2017, 44, 1079-1087.	4.0	44
46	Potential of Aerosol Liquid Water to Facilitate Organic Aerosol Formation: Assessing Knowledge Gaps about Precursors and Partitioning. Environmental Science & Technology, 2017, 51, 3327-3335.	10.0	55
47	Can COSMOTherm Predict a Salting in Effect?. Journal of Physical Chemistry A, 2017, 121, 6288-6295.	2.5	17
48	Formaldehyde in the Tropical Western Pacific: Chemical Sources and Sinks, Convective Transport, and Representation in CAMâ€Chem and the CCMI Models. Journal of Geophysical Research D: Atmospheres, 2017, 122, 11201-11226.	3.3	32
49	BrO and inferred Br _{<i>y</i>} profiles over the western Pacific: relevance of inorganic bromine sources and a Br _{<i>y</i>} minimum in the aged tropical tropopause laver. Atmospheric Chemistry and Physics. 2017. 17. 15245-15270.	4.9	33
50	Investigating differences in DOAS retrieval codes using MAD-CAT campaign data. Atmospheric Measurement Techniques, 2017, 10, 955-978.	3.1	20
51	New Measurements of the Rate Constants of the Reactions of Pentenal, Hexenal, Heptenal, and Nonenal with Ozone, OH Radicals, and Br Atoms. , 2017, , .		0
52	MAX-DOAS measurements of HONO slant column densities during the MAD-CAT campaign: inter-comparison, sensitivity studies on spectral analysis settings, and error budget. Atmospheric Measurement Techniques, 2017, 10, 3719-3742.	3.1	31
53	The CU mobile Solar Occultation Flux instrument: structure functions and emission rates of NH ₃ , NO ₂ and C ₂ H ₆ . Atmospheric Measurement Techniques. 2017. 10. 373-392.	3.1	22
54	Recent advances in understanding secondary organic aerosol: Implications for global climate forcing. Reviews of Geophysics, 2017, 55, 509-559.	23.0	548

#	Article	IF	CITATIONS
55	Maximizing Degrees of Freedom in MAX-DOAS Retrievals of BrO from Remote Tropical Marine Mountaintops. , 2017, , .		1
56	Emission Fluxes from Agricultural Sources and Biomass Burning using the CU Airborne SOF Instrument. , 2017, , .		0
57	Development of a digital mobile solar tracker. Atmospheric Measurement Techniques, 2016, 9, 963-972.	3.1	13
58	Parameterization retrieval of trace gas volume mixing ratios from Airborne MAX-DOAS. Atmospheric Measurement Techniques, 2016, 9, 5655-5675.	3.1	19
59	Observational constraints on glyoxal production from isoprene oxidation and its contribution to organic aerosol over the Southeast United States. Journal of Geophysical Research D: Atmospheres, 2016, 121, 9849-9861.	3.3	48
60	Model representations of aerosol layers transported from North America over the Atlantic Ocean during the Two olumn Aerosol Project. Journal of Geophysical Research D: Atmospheres, 2016, 121, 9814-9848.	3.3	15
61	Modeling the weekly cycle of NO _x and CO emissions and their impacts on O ₃ in the Los Angelesâ€6outh Coast Air Basin during the CalNex 2010 field campaign. Journal of Geophysical Research D: Atmospheres, 2016, 121, 1340-1360.	3.3	51
62	Measurements of hydroxyl and hydroperoxy radicals during CalNex‣A: Model comparisons and radical budgets. Journal of Geophysical Research D: Atmospheres, 2016, 121, 4211-4232.	3.3	81
63	Characterization of Chromophoric Water-Soluble Organic Matter in Urban, Forest, and Marine Aerosols by HR-ToF-AMS Analysis and Excitation–Emission Matrix Spectroscopy. Environmental Science & Technology, 2016, 50, 10351-10360.	10.0	139
64	The Two olumn Aerosol Project: Phase I—Overview and impact of elevated aerosol layers on aerosol optical depth. Journal of Geophysical Research D: Atmospheres, 2016, 121, 336-361.	3.3	33
65	Modeling the observed tropospheric BrO background: Importance of multiphase chemistry and implications for ozone, OH, and mercury. Journal of Geophysical Research D: Atmospheres, 2016, 121, 11,819.	3.3	106
66	An assessment of the radiative effects of ice supersaturation based on in situ observations. Geophysical Research Letters, 2016, 43, 11,039.	4.0	8
67	Heterogeneous photochemistry of imidazole-2-carboxaldehyde: HO ₂ radical formation and aerosol growth. Atmospheric Chemistry and Physics, 2016, 16, 11823-11836.	4.9	48
68	Global impacts of tropospheric halogens (Cl, Br, I) on oxidants and composition in GEOS-Chem. Atmospheric Chemistry and Physics, 2016, 16, 12239-12271.	4.9	231
69	Mercury oxidation from bromine chemistry in the free troposphere over the southeasternÂUS. Atmospheric Chemistry and Physics, 2016, 16, 3743-3760.	4.9	33
70	lodine's impact on tropospheric oxidants: aÂglobal model study in GEOS-Chem. Atmospheric Chemistry and Physics, 2016, 16, 1161-1186.	4.9	116
71	Aqueous phase oxidation of sulphur dioxide by ozone in cloud droplets. Atmospheric Chemistry and Physics, 2016, 16, 1693-1712.	4.9	47
72	First detection of ammonia (NH ₃) in the Asian summer monsoon upper troposphere. Atmospheric Chemistry and Physics, 2016, 16, 14357-14369.	4.9	51

#	Article	IF	CITATIONS
73	Contribution of dissolved organic matter to submicron water-soluble organic aerosols in the marine boundary layer over the eastern equatorial Pacific. Atmospheric Chemistry and Physics, 2016, 16, 7695-7707.	4.9	24
74	Elevated aerosol layers modify the O2–O2 absorption measured by ground-based MAX-DOAS. Journal of Quantitative Spectroscopy and Radiative Transfer, 2016, 176, 34-49.	2.3	22
75	The CU 2-D-MAX-DOAS instrument – Part 2: Raman scattering probability measurements and retrieval of aerosol optical properties. Atmospheric Measurement Techniques, 2016, 9, 3893-3910.	3.1	8
76	Injection of iodine to the stratosphere. Geophysical Research Letters, 2015, 42, 6852-6859.	4.0	52
77	Weakening of the weekend ozone effect over California's South Coast Air Basin. Geophysical Research Letters, 2015, 42, 9457-9464.	4.0	32
78	The CU 2-D-MAX-DOAS instrument – Part 1: Retrieval of 3-D distributions of NO ₂ and azimuth-dependent OVOC ratios. Atmospheric Measurement Techniques, 2015, 8, 2371-2395.	3.1	39
79	Ground-based direct-sun DOAS and airborne MAX-DOAS measurements of the collision-induced oxygen complex, O _{2_{, absorption with significant pressure and temperature differences. Atmospheric Measurement Techniques, 2015, 8, 793-809.}}	3.1	26
80	Computational Study of the Effect of Glyoxal–Sulfate Clustering on the Henry's Law Coefficient of Glyoxal. Journal of Physical Chemistry A, 2015, 119, 4509-4514.	2.5	35
81	Measurements of the Absorption Cross Section of ¹³ CHO ¹³ CHO at Visible Wavelengths and Application to DOAS Retrievals. Journal of Physical Chemistry A, 2015, 119, 4651-4657.	2.5	0
82	Active and widespread halogen chemistry in the tropical and subtropical free troposphere. Proceedings of the National Academy of Sciences of the United States of America, 2015, 112, 9281-9286.	7.1	91
83	A Tribute to Mario Molina. Journal of Physical Chemistry A, 2015, 119, 4277-4278.	2.5	2
84	Aircraft measurements of BrO, IO, glyoxal, NO ₂ , H ₂ O, O ₂ –O ₂ and aerosol extinction profiles in the tropics: comparison with aircraft-/ship-based in situ and lidar	3.1	107
85	measurements. Atmospheric Measurement Techniques, 2015, 8, 2121-2148. Instrument intercomparison of glyoxal, methyl glyoxal and NO ₂ under simulated atmospheric conditions. Atmospheric Measurement Techniques, 2015, 8, 1835-1862.	3.1	50
86	Glyoxal and Methylglyoxal Setschenow Salting Constants in Sulfate, Nitrate, and Chloride Solutions: Measurements and Gibbs Energies. Environmental Science & Technology, 2015, 49, 11500-11508.	10.0	64
87	Measurements of diurnal variations and eddy covariance (EC) fluxes of glyoxal in the tropical marine boundary layer: description of the Fast LED-CE-DOAS instrument. Atmospheric Measurement Techniques, 2014, 7, 3579-3595.	3.1	49
88	Rayleigh scattering cross-section measurements of nitrogen, argon, oxygen and air. Journal of Quantitative Spectroscopy and Radiative Transfer, 2014, 147, 171-177.	2.3	101
89	Formation of gas-phase carbonyls from heterogeneous oxidation of polyunsaturated fatty acids at the air–water interface and of the sea surface microlayer. Atmospheric Chemistry and Physics, 2014, 14, 1371-1384.	4.9	62
90	Simulation of semi-explicit mechanisms of SOA formation from glyoxal in aerosol in a 3-D model. Atmospheric Chemistry and Physics, 2014, 14, 6213-6239.	4.9	166

#	Article	IF	CITATIONS
91	Novel Pathways to Form Secondary Organic Aerosols: Glyoxal SOA in WRF/Chem. Springer Proceedings in Complexity, 2014, , 149-154.	0.3	0
92	Temperature dependent absorption cross-sections of O2–O2 collision pairs between 340 and 630 nm and at atmospherically relevant pressure. Physical Chemistry Chemical Physics, 2013, 15, 15371.	2.8	305
93	The 2010 California Research at the Nexus of Air Quality and Climate Change (CalNex) field study. Journal of Geophysical Research D: Atmospheres, 2013, 118, 5830-5866.	3.3	199
94	Effective Henry's Law Partitioning and the Salting Constant of Glyoxal in Aerosols Containing Sulfate. Environmental Science & Technology, 2013, 47, 4236-4244.	10.0	115
95	Parameterizing radiative transfer to convert MAX-DOAS dSCDs into near-surface box-averaged mixing ratios. Atmospheric Measurement Techniques, 2013, 6, 1521-1532.	3.1	32
96	The CU Airborne MAX-DOAS instrument: vertical profiling of aerosol extinction and trace gases. Atmospheric Measurement Techniques, 2013, 6, 719-739.	3.1	86
97	Detection of iodine monoxide in the tropical free troposphere. Proceedings of the National Academy of Sciences of the United States of America, 2013, 110, 2035-2040.	7.1	88
98	Organic aerosol composition and sources in Pasadena, California, during the 2010 CalNex campaign. Journal of Geophysical Research D: Atmospheres, 2013, 118, 9233-9257.	3.3	231
99	Secondary organic aerosol formation from semi―and intermediateâ€volatility organic compounds and glyoxal: Relevance of O/C as a tracer for aqueous multiphase chemistry. Geophysical Research Letters, 2013, 40, 978-982.	4.0	69
100	Airborne MAXâ€ÐOAS measurements over California: Testing the NASA OMI tropospheric NO ₂ product. Journal of Geophysical Research D: Atmospheres, 2013, 118, 7400-7413.	3.3	26
101	Overview of the 2010 Carbonaceous Aerosols and Radiative Effects Study (CARES). Atmospheric Chemistry and Physics, 2012, 12, 7647-7687.	4.9	94
102	Modeling the Multiday Evolution and Aging of Secondary Organic Aerosol During MILAGRO 2006. Environmental Science & Technology, 2011, 45, 3496-3503.	10.0	90
103	Detailed comparisons of airborne formaldehyde measurements with box models during the 2006 INTEX-B and MILACRO campaigns: potential evidence for significant impacts of unmeasured and multi-generation volatile organic carbon compounds. Atmospheric Chemistry and Physics, 2011, 11, 11867-11894.	4.9	46
104	The CU ground MAX-DOAS instrument: characterization of RMS noise limitations and first measurements near Pensacola, FL of BrO, IO, and CHOCHO. Atmospheric Measurement Techniques, 2011, 4, 2421-2439.	3.1	57
105	Impacts of HONO sources on the photochemistry in Mexico City during the MCMA-2006/MILAGO Campaign. Atmospheric Chemistry and Physics, 2010, 10, 6551-6567.	4.9	222
106	Oxidative capacity of the Mexico City atmosphere – Part 2: A RO _x radical cycling perspective. Atmospheric Chemistry and Physics, 2010, 10, 6993-7008.	4.9	64
107	An overview of the MILAGRO 2006 Campaign: Mexico City emissions and their transport and transformation. Atmospheric Chemistry and Physics, 2010, 10, 8697-8760.	4.9	349
108	Ship-based detection of glyoxal over the remote tropical Pacific Ocean. Atmospheric Chemistry and Physics, 2010, 10, 11359-11371.	4.9	125

#	Article	IF	CITATIONS
109	Ozone response to emission changes: a modeling study during the MCMA-2006/MILAGRO Campaign. Atmospheric Chemistry and Physics, 2010, 10, 3827-3846.	4.9	73
110	Mexico city aerosol analysis during MILAGRO using high resolution aerosol mass spectrometry at the urban supersite (TO) – Part 2: Analysis of the biomass burning contribution and the non-fossil carbon fraction. Atmospheric Chemistry and Physics, 2010, 10, 5315-5341.	4.9	182
111	Oxidative capacity of the Mexico City atmosphere – Part 1: A radical source perspective. Atmospheric Chemistry and Physics, 2010, 10, 6969-6991.	4.9	146
112	Glyoxal processing by aerosol multiphase chemistry: towards a kinetic modeling framework of secondary organic aerosol formation in aqueous particles. Atmospheric Chemistry and Physics, 2010, 10, 8219-8244.	4.9	320
113	Inherent calibration of a blue LED-CE-DOAS instrument to measure iodine oxide, glyoxal, methyl glyoxal, nitrogen dioxide, water vapour and aerosol extinction in open cavity mode. Atmospheric Measurement Techniques, 2010, 3, 1797-1814.	3.1	135
114	Implications of the Inâ€Situ Measured Mass Absorption Cross Section of Organic Aerosols in Mexico City on the Atmospheric Energy Balance, Satellite Retrievals, and Photochemistry. , 2009, , .		2
115	Dealkylation of Alkylbenzenes: A Significant Pathway in the Toluene, <i>o</i> -, <i>m</i> -, <i>p</i> -Xylene + OH Reaction. Journal of Physical Chemistry A, 2009, 113, 9658-9666.	2.5	49
116	Light emitting diode cavity enhanced differential optical absorption spectroscopy (LED-CE-DOAS): a novel technique for monitoring atmospheric trace gases. , 2009, , .		2
117	Impact of primary formaldehyde on air pollution in the Mexico City Metropolitan Area. Atmospheric Chemistry and Physics, 2009, 9, 2607-2618.	4.9	70
118	Evaluation of recently-proposed secondary organic aerosol models for a case study in Mexico City. Atmospheric Chemistry and Physics, 2009, 9, 5681-5709.	4.9	261
119	Measurements of OH and HO ₂ concentrations during the MCMA-2006 field campaign – Part 1: Deployment of the Indiana University laser-induced fluorescence instrument. Atmospheric Chemistry and Physics, 2009, 9, 1665-1685.	4.9	104
120	Secondary Organic Aerosol Formation from Acetylene (C ₂ H ₂): seed effect on SOA yields due to organic photochemistry in the aerosol aqueous phase. Atmospheric Chemistry and Physics, 2009, 9, 1907-1928.	4.9	329
121	Measurements of Volatile Organic Compounds Using Proton Transfer Reaction – Mass Spectrometry during the MILAGRO 2006 Campaign. Atmospheric Chemistry and Physics, 2009, 9, 467-481.	4.9	79
122	Mexico City aerosol analysis during MILAGRO using high resolution aerosol mass spectrometry at the urban supersite (T0) – Part 1: Fine particle composition and organic source apportionment. Atmospheric Chemistry and Physics, 2009, 9, 6633-6653.	4.9	525
123	Measurements of OH and HO ₂ concentrations during the MCMA-2006 field campaign – Part 2: Model comparison and radical budget. Atmospheric Chemistry and Physics, 2009, 9, 6655-6675.	4.9	105
124	MAX-DOAS observations from ground, ship, and research aircraft: maximizing signal-to-noise to measure 'weak' absorbers. , 2009, , .		20
125	The influence of natural and anthropogenic secondary sources on the glyoxal global distribution. Atmospheric Chemistry and Physics, 2008, 8, 4965-4981.	4.9	174
126	Estimation of the mass absorption cross section of the organic carbon component of aerosols in the Mexico City Metropolitan Area. Atmospheric Chemistry and Physics, 2008, 8, 6665-6679.	4.9	137

#	Article	IF	CITATIONS
127	Measurements of HNO ₃ and N ₂ O ₅ using ion drift-chemical ionization mass spectrometry during the MILAGRO/MCMA-2006 campaign. Atmospheric Chemistry and Physics, 2008, 8, 6823-6838.	4.9	83
128	Characterizing ozone production and response under different meteorological conditions in Mexico City. Atmospheric Chemistry and Physics, 2008, 8, 7571-7581.	4.9	55
129	Modelling constraints on the emission inventory and on vertical dispersion for CO and SO ₂ in the Mexico City Metropolitan Area using Solar FTIR and zenith sky UV spectroscopy. Atmospheric Chemistry and Physics, 2007, 7, 781-801.	4.9	82
130	Characterizing ozone production in the Mexico City Metropolitan Area: a case study using a chemical transport model. Atmospheric Chemistry and Physics, 2007, 7, 1347-1366.	4.9	154
131	Evaluation of nitrogen dioxide chemiluminescence monitors in a polluted urban environment. Atmospheric Chemistry and Physics, 2007, 7, 2691-2704.	4.9	343
132	Distribution, magnitudes, reactivities, ratios and diurnal patterns of volatile organic compounds in the Valley of Mexico during the MCMA 2002 & 2003 field campaigns. Atmospheric Chemistry and Physics, 2007, 7, 329-353.	4.9	167
133	MAX-DOAS detection of glyoxal during ICARTT 2004. Atmospheric Chemistry and Physics, 2007, 7, 1293-1303.	4.9	78
134	A missing sink for gasâ€phase glyoxal in Mexico City: Formation of secondary organic aerosol. Geophysical Research Letters, 2007, 34, .	4.0	415
135	Secondary organic aerosol formation from anthropogenic air pollution: Rapid and higher than expected. Geophysical Research Letters, 2006, 33, .	4.0	1,027
136	Simultaneous global observations of glyoxal and formaldehyde from space. Geophysical Research Letters, 2006, 33, .	4.0	265
137	Atmospheric oxidation in the Mexico City Metropolitan Area (MCMA) during April 2003. Atmospheric Chemistry and Physics, 2006, 6, 2753-2765.	4.9	204
138	Technical note: Evaluation of standard ultraviolet absorption ozone monitors in a polluted urban environment. Atmospheric Chemistry and Physics, 2006, 6, 3163-3180.	4.9	37
139	Implementation of a Markov Chain Monte Carlo method to inorganic aerosol modeling of observations from the MCMA-2003 campaign – PartÂII: Model application to the CENICA, Pedregal and Santa Ana sites. Atmospheric Chemistry and Physics, 2006, 6, 4889-4904.	4.9	34
140	Separation of emitted and photochemical formaldehyde in Mexico City using a statistical analysis and a new pair of gas-phase tracers. Atmospheric Chemistry and Physics, 2006, 6, 4545-4557.	4.9	146
141	Characterization of ambient aerosols in Mexico City during the MCMA-2003 campaign with Aerosol Mass Spectrometry: results from the CENICA Supersite. Atmospheric Chemistry and Physics, 2006, 6, 925-946.	4.9	341
142	Intercomparison of the DOAS and LOPAP techniques for the detection of nitrous acid (HONO). Atmospheric Environment, 2006, 40, 3640-3652.	4.1	152
143	Remote Sensing of Glyoxal by Differential Optical Absorption Spectroscopy (DOAS): Advancements in Simulation Chamber and Field Experiments. , 2006, , 129-141.		8
144	Intercomparison of four different in-situ techniques for ambient formaldehyde measurements in urban air. Atmospheric Chemistry and Physics, 2005, 5, 2881-2900.	4.9	148

#	Article	IF	CITATIONS
145	Development of a detailed chemical mechanism (MCMv3.1) for the atmospheric oxidation of aromatic hydrocarbons. Atmospheric Chemistry and Physics, 2005, 5, 641-664.	4.9	442
146	High-resolution absorption cross-section of glyoxal in the UV–vis and IR spectral ranges. Journal of Photochemistry and Photobiology A: Chemistry, 2005, 172, 35-46.	3.9	218
147	DOAS measurement of glyoxal as an indicator for fast VOC chemistry in urban air. Geophysical Research Letters, 2005, 32, .	4.0	211
148	Fast gas chromatography with luminol chemiluminescence detection for the simultaneous determination of nitrogen dioxide and peroxyacetyl nitrate in the atmosphere. Review of Scientific Instruments, 2004, 75, 4595-4605.	1.3	34
149	OH-initiated oxidation of benzene. Physical Chemistry Chemical Physics, 2002, 4, 4399-4411.	2.8	65
150	OH-initiated oxidation of benzene. Physical Chemistry Chemical Physics, 2002, 4, 1598-1610.	2.8	159
151	Primary and Secondary Clyoxal Formation from Aromatics:  Experimental Evidence for the Bicycloalkylâ^'Radical Pathway from Benzene, Toluene, and p-Xylene. Journal of Physical Chemistry A, 2001, 105, 7865-7874.	2.5	263
152	Correction of the oxygen interference with UV spectroscopic (DOAS) measurements of monocyclic aromatic hydrocarbons in the atmosphere. Atmospheric Environment, 1998, 32, 3731-3747.	4.1	77
153	Atmospheric Oxidation of Toluene in a Large-Volume Outdoor Photoreactor:Â In Situ Determination of Ring-Retaining Product Yields. Journal of Physical Chemistry A, 1998, 102, 10289-10299.	2.5	136